

VIP Very Important Paper

Special
Collection

Reactions in Endohedral Functionalized Cages

Matthias Otte*^[a]

The introduction of enhanced functionalization is a key aspect in the current design of cage chemistry. At the moment, several approaches are intensively investigated. The synthesis of cage compounds that display endohedral functionalization plays a key role among them. Here, the studies of reactions that occur in endohedral-functionalized cage compounds is reviewed. After an introduction in current trends in cage-chemistry the discussion of reactions in endohedral-cage compounds is

divided into three sections. These are: 1) Endohedral groups that are by themselves functional, 2) endohedral groups that can bind to a transition-metal complex and 3) endohedral groups that can bind by themselves to a metal. The article closes with an outlook on additional current developments in the field of endohedral-functionalized cage-compounds, which may contribute in the future towards reactivity in cage compounds.

1. Introduction

Cage and capsule compounds have proven their ability to mediate or catalyze chemical reactions. These so-called molecular flasks have demonstrated to impact the reaction outcome in a way, which often cannot be achieved without the cage or capsule present.

The regioselectivity of a reaction can be different inside a cage when compared to the reaction in bulk solution. Taking Diels–Alder reactions as an example, this has been demonstrated by Fujita.^[1] Rebek reported on selective macrocyclization using a cavitand that causes folding of the diamine substrates.^[2] Cages can alter the properties of encapsulated guests. Raymond and Bergman demonstrated that encapsulated orthoformates change drastically their pK_A values, which enables an acid catalysis hydrolysis in basic solution.^[3]

Due to their limited pore sizes, cage compounds can selectively convert substrates based on their size or positioning of their functional groups, leading to size-, site- or substrate-selective reactions. Tiefenbacher demonstrated the size-selective hydrolysis of diethyl acetals that is catalyzed by a resorcin[4]arene capsule.^[4] Raymond, Bergman and Toste reported on the encapsulation of a rhodium based hydrogenation catalyst in a supramolecular cage. This system is capable to selectively hydrogenate one carbon-carbon double bond, even if multiple alkene functionalities are present in the substrate.^[5] This system can also differentiate between two substrates when they possess carbon-carbon double bonds in different distance to the terminal carbon.

Supramolecular hosts can protect an encapsulated catalyst from certain deactivation pathways. Nguyen and Hupp reported on a molecular square built of porphyrins, which is able to protect an encapsulated manganese porphyrin. The manganese porphyrin is an epoxidation catalyst, which undergoes deactivation via formation of an oxo-bridged dimer when it is not encapsulated.^[6] This concept has been used by de Bruin to protect cobalt and manganese porphyrins in a cubic M₈L₆ Nitschke-type cage.^[7–8] Raymond and Bergman demonstrated that catalyst encapsulation can also result in catalyst protection from substrates that would cause inhibition while other substrates can be converted at the same time. This has been shown for the rhodium catalyzed isomerization of allylic alcohols.^[9]

Most molecular flasks described in the literature are highly symmetric compounds (Figure 1, top). Such symmetric compounds are often obtained as the thermodynamic products via metal-ligand coordination, supramolecular interactions such as hydrogen bonding or dynamic combinatorial chemistry.^[10–12] These compounds possess often aromatic walls and in case of species that assemble via metal-ligand coordination also high

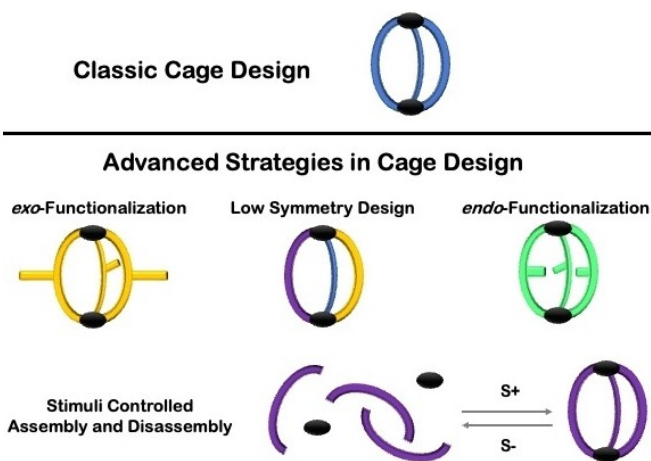


Figure 1. Approaches to advanced cage functionality.

[a] Dr. M. Otte
Institute of Inorganic Chemistry
University of Goettingen
Tammannstraße 4, 37077 Göttingen (Germany)
E-mail: matthias.otte@chemie.uni-goettingen.de

This article belongs to a Joint Special Collection dedicated to Ulf Diederichsen.

© 2023 The Authors. European Journal of Organic Chemistry published by Wiley-VCH GmbH. This is an open access article under the terms of the Creative Commons Attribution License, which permits use, distribution and reproduction in any medium, provided the original work is properly cited.

charges. In recent years, the field of cage design expanded to new synthetic strategies with the aim to add functionalities to the molecular flasks.

One approach is the introduction of exohedral functionalization to cages (Figure 1, left). Such *exo*-groups can impact the solubility of the cage assembly. Casini and Kühn studied *exo*-CH₂OH-functionalized Pd₂L₄ cages as delivery vehicles for the anticancer drug cisplatin.^[13] *exo*-Functionalization may also be used to connect cages. Clever reported on the use of banana shape ligands that are connected via a linker to synthesize [Pd₄L¹₂L²₄] dimeric cages that consist of two linked cages.^[14] Exohedral functionalization may also be used to build a cage around a cage as shown by Fujita.^[15] This however, might also be seen as an endohedral functionalization that results in the formation of a cage in a cage. The connection of cages via exohedral functionalization may also result in the formation of polymeric structures. Bloch demonstrated the synthesis of amine-functionalized Cu₂₄L₂₄ cages that turn into gels upon dialdehyde addition.^[16] The connection of organic cages via organic linkers can lead to the formation of cage based covalent organic frameworks. Examples of such frameworks have been reported by Wang or Chen, Little and Cooper.^[17,18] In addition to the formation of frameworks, *exo*-functionalization can also be used to assemble so-called cage-dumbbells. Greenaway reported the formation of organic cage dumbbells, while Roemelt and Otte showed a cage dumbbell that uses an Fe(terpy)₂ moiety as connecting unit.^[19,20]

A different approach to increase functionality is the selective synthesis of cages with lower symmetry (Figure 1, centre). These compounds are often difficult to obtain selectively as their formation competes with scrambling processes. However, significant progress has been made in this field within the last years. Mukherjee showed the selective synthesis of a cage with a Pd₇ boat structure that self-assembles from a reaction mixture containing tri- and tetra-imidazole donors.^[21] The obtained cage is able to catalyze Knoevenagel condensation reactions. Clever reported the selective synthesis of heteroleptic [Pd₂L¹₂L²₂] cages via the use of different bis-monodentate pyridyl ligands that possess different bite angles.^[22] Severin demonstrated the synthesis of a [Pd₁₂L₂₄] sphere by using an unsymmetric 3-(4-(pyridin-4-yl)phenyl)pyridine ligand. Remarkably, one cage is

selectively obtained out of 350696 isomers.^[23] Beuerle showed that social self-sorting could be achieved for the construction of three-component cages of the A₄B₄C₂ type with A being a compound with three catechol units and B and C are diboronic acids with bite angles of 120° and 180°.^[24] Mastalerz showed examples of social-self-sorting of different building blocks that result in the same cage geometries. Within these studies [2 + 3] and [8 + 12] salicylimine cage compounds have been selectively obtained.^[25]

Within the recent years, examples emerged that show the possibility to selectively assemble and disassemble supramolecular structures based on external stimuli (Figure 1, bottom). Goeb and Sallé presented cages that are assembled from pyridine coordination of building blocks containing extended tetrathiafulvalene units.^[26] Such building blocks undergo conformational changes upon oxidation leading to a disassembly of the cage. This process is reversible and a reassembly is observed upon reduction. Nitschke showed that a supramolecular triangular receptor, suitable to encapsulate C₆₀ can be disrupted upon addition of triphenylphosphine. Triphenylphosphine competes with the *N,N*-bidentate chelating units of the receptor for the structure giving copper. Addition of a *N*-oxide and an oxo-transfer catalysts results in the formation of the OPPh₃, causing the reassembly of the supramolecular receptor.^[27]

The combination of photochemistry and supramolecular assembly and disassembly processes is a particular field that receives currently much attention. Clever showed a coordination cage based on a ligand embedding a diazocine photo-switch. The thermodynamic more stable *cis*-isomer assembles to a mixture of species upon palladium coordination, while the less stable *trans*-isomer gives a [Pd₂*trans*-L₄] cage. That cage is only stable under UV light and in the absence of this stimulus the system converts into the *cis*-system.^[28] Schmidt combined light switchable azobenzenes and imine condensations to macrocycles resulting in a photoresponsive and dissipative dynamic covalent macrocycle.^[29] Beves introduced a photoswitchable ligand allowing to switch between a [Pd₂L₄] cage and a [PdL₂] species.^[30] McConnell and Herges introduced a mixture of regioisomeric diazocine ligands that can switch between the *E*- and *Z*-configuration each upon irradiation with violet and green light. Upon switching to the *Z*-form, one ligand forms a Co₂(L-*Z*)₃ species, while the other forms a mixture of oligomers. Switching to the *E*-form, the opposite was observed. The ligand that gave oligomers with the *Z*-form results now in the formation of a Co₂(L-*E*)₃ species.^[31]

After this brief overview on current developments for an enhanced functionalization of supramolecular cage compounds, the focus should now lie on an additional way to bring function into cage chemistry. That is the introduction of endohedral-functionalization into the cage cavities (Figure 1, right). Such *endo*-functionalization may serve different purposes, like sensing of compounds or to mediate or catalyze chemical reactions. The *endo*-group can be functional by itself or bind to a functional group of a guest molecule or guest complex. The functional group may also serve directly as a ligand. In particular, the developments of *endo*-functionalized cages with



Matthias Otte studied chemistry at Bonn University. He obtained his Ph.D. in 2011 under the supervision of Andreas Gansäuer from the same university. He did his postdoctoral studies in the group of Bas de Bruin at the University of Amsterdam. In 2013, he joined the Organic Chemistry and Catalysis group at Utrecht University. In 2017, he moved to Göttingen University where he is currently a group leader. Matthias Otte obtained a Chemiefonds-Scholarship of the Fonds der Chemischen Industrie and a Feodor Lynen-Scholarship of the Alexander von Humboldt-Foundation. His research interests are in the fields of supramolecular chemistry, bio-inorganic chemistry and catalysis.

respect to mediating or catalyzing reactions will be discussed here. Hooley reviewed the synthesis and application of *endo*-functionalized metal-ligand cage complexes in 2019.^[32]

Here, the scope is extended to organic cage compounds and also the development in recent years will be included. The examples being discussed will be ordered regarding the role that the *endo*-group plays. It will start with systems where the *endo*-group by itself will be functional in terms of mediating or catalyzing reactions. It will continue with a section on endohedral-functionalized systems that can bind to a complex ligand and afterwards a section follows where the endohedral-functionalized cages act by themselves as ligands. The manuscript closes with an outlook where also other developments of endohedral-functionalized cages are mentioned, which may contribute in the future to cage catalysis.

2. Endohedral Group is Functional by Itself

Endohedral functionalization was long time seen as to be too difficult to be achieved with synthetic supramolecular cage compounds. The reason given was that such cavities would be too small to host *endo*-groups. Fujita demonstrated in 2005 that $M_{12}L_{24}^{24+}$ spheres (**1**) that assemble from Pd^{2+} ions and bis(4-pyridyl)-functionalized building blocks (**2**) are suitable for *endo*-functionalization (Figure 2; left).^[33] Within this study, several spheres have been reported with different functionalized building blocks, ranging from a CH_3 -group (**1a**) to an oligo(ethylene oxide) chain (**1b**). The later one has been shown to be capable of encapsulating La(III) ions with a ratio of roughly 1:1 of La(III) to *endo*-group, leading to a species with around 20 La(III) ions in the spheres cavity. In a later study, Fujita showed that also 24 methyl methacrylate units can be included in these types of spheres (**1c**) (Figure 2).^[34] Using 2,2'-azobis(isobutyronitrile) (AIBN) as radical initiator, conversions of up 73% were obtained for the endohedral radical polymer-

ization. After hydrolysis, gel permeation chromatography reveals a number-average molecular weight of 1315 and a polydispersity index of 1.60. In a following study, Fujita employed glucose functionalized building blocks (**1d**) to obtain spheres capable to act as templates for the sol-gel condensation of alkoxy silanes leading to monodisperse silica nanoparticles.^[35]

The $M_{12}L_{24}$ complexes are once formed stable and ligand exchange between different spheres seems to occur only very slowly on a time scale of weeks or months. This advantage has been used by Fujita to place two catalysts that would react with each other in two different $M_{12}L_{24}$ spheres. The unusual functional group tolerance has been achieved via connecting each catalyst via a linker to a bis(4-pyridyl)-functionalized building block resulting in two different *endo*-functionalized spheres (Figure 3).^[36] Connecting TEMPO to such a building block resulted in **3a** that after reaction with Pd^{2+} ions gives **4a** while connection of MacMillan's enantioselective Diels–Alder catalyst resulted after reaction with Pd^{2+} ions in the self-assembly of **4b**.^[37] In the absence of any sphere-protection, the TEMPO-catalyst would oxidize the Diels–Alder-catalyst (Figure 3, box). This could be prevented by containing each catalyst in the corresponding sphere during the reaction. In this regard, it was possible to have a one batch reaction going from the alcohol **5** via oxidation to aldehyde **6** to the enantiomeric enriched Diels–Alder-reaction product **7**. Given that under normal circumstances individual reaction set-up with following work-up and purification after each step is time and material consuming, this study is a conceptual approach how multistep cascade processes might be realized in a one-pot procedure via the help of supramolecular chemistry.

The bis(4-pyridyl) building blocks leading to $M_{12}L_{24}$ spheres can be functionalized in a broad range. As such, the resulting spheres can be *endo*- or *exo*-functionalized.^[38] Recently, Oldenhuis and Johnson combined different building blocks leading to *endo*- and *exo*-functionalization of spheres.^[39] The *exo*-

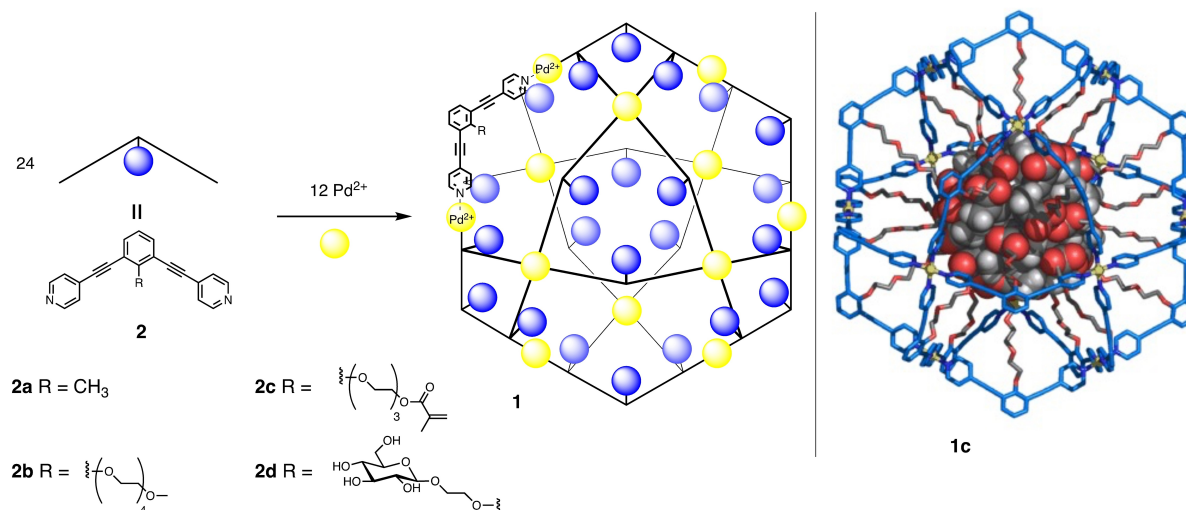


Figure 2. Left: Assembly of *endo*-functionalized $M_{12}L_{24}^{24+}$ spheres from Pd^{2+} ions and bis(4-pyridyl)-functionalized building blocks;^[33–35] right: Molecular model of **1c**. Reproduced from Ref. [34] Copyright (2007), with permission from Wiley-VCH.

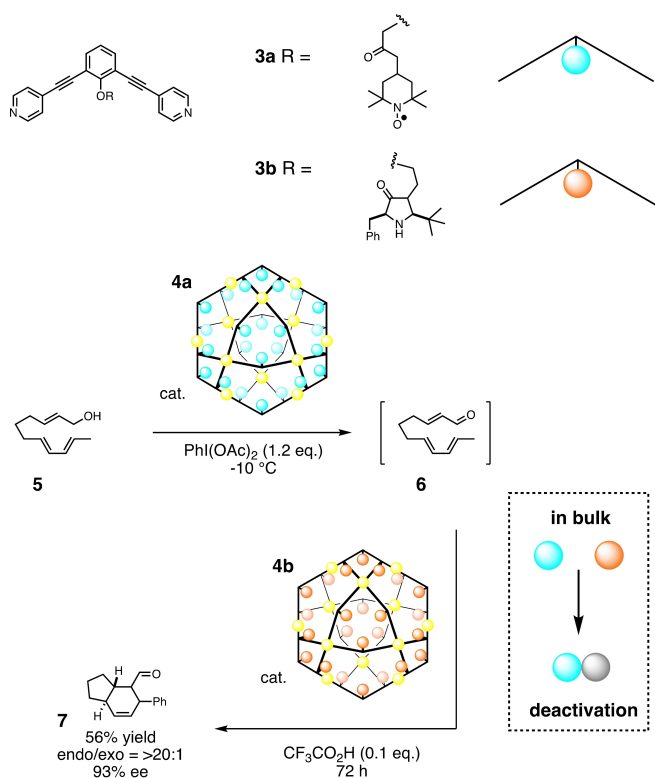


Figure 3. $M_{12}L_{24}^{24+}$ spheres for a site-isolation strategy leading to new cascade reactions. The cascade consists of a TEMPO-catalyzed alcohol oxidation and an asymmetric Diels–Alder reaction.^[36]

building blocks link thereby several 1,3-bis(pyridin-4-ylethynyl)benzene units. This causes the formation of gel like polymeric structures where the physical properties of the gel are determined on the ratio of the *endo*- and *exo*-building blocks that are applied and which *exo*-building block is used. This approach aims to combine the advantages of swollen gels such as a great reagent mobility with those of crystalline, porous polymers (e.g. metal–organic frameworks; MOFs) which is the exquisite local tuning of catalyst environment. A precursor to the *endo*-functionalized spheres that has been used is **8** (Figure 4). This can be combined with the already introduced TEMPO-functionalized building block **3a**, leading to gels of the type **9** (Figure 4 top). The obtained gels **9** have been shown to catalyze the oxidation of alcohol **10** to aldehyde **11** (Figure 4 bottom). The oxidation of **10** occurs in the presence of **9** in a similar rate as it happens in the presence of **3a**. Further, **9** can be recycled and maintains its performance for five cycles (conversion > 95%).

Hooley introduced the $M_4L_6^{8+}$ cage **12**, which has carboxylic acid groups as *endo*-functionalization (Figure 5).^[40] That compound is obtained via self-assembly from an extended 2,7-dianilino-fluorene (**13**), 2-formylpyridine (**14**) and Fe(NTf₂)₂. **12** is able to catalyze the hydrolysis of acetals at room temperature (Figure 6a). Apparently, the cage is needed around the carboxylic acid groups as the control carboxylic acid-functionalized compound (**15**; Figure 5, box) is not capable to perform the catalysis under the cage operating conditions. Further, the

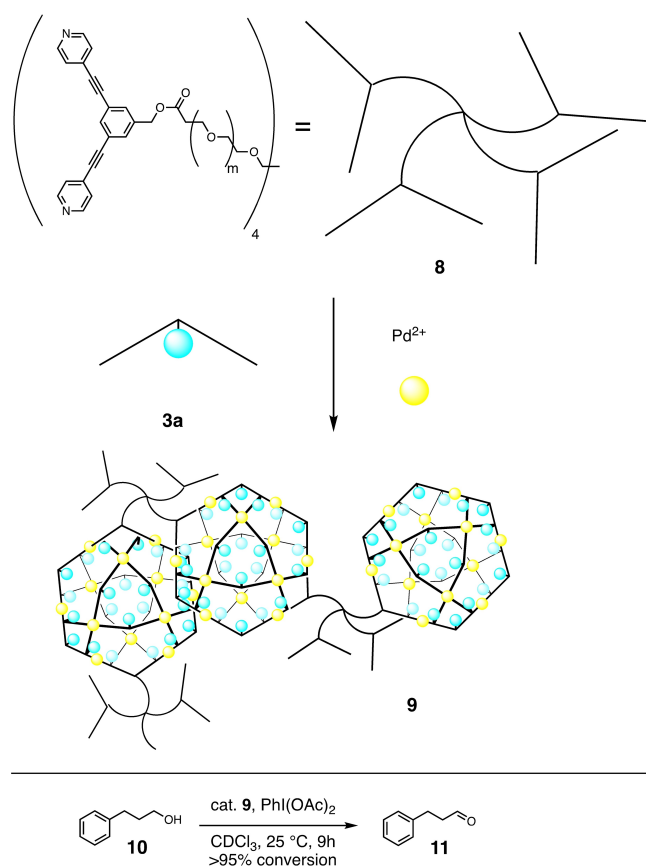


Figure 4. Top: Schematic depiction of the synthesis of $M_{12}L_{24}^{24+}$ sphere-based gels **9** via combination of **3a** and **8**. Bottom: Application of $M_{12}L_{24}^{24+}$ sphere-based gels as catalysts for the oxidation of alcohols to aldehydes.^[39]

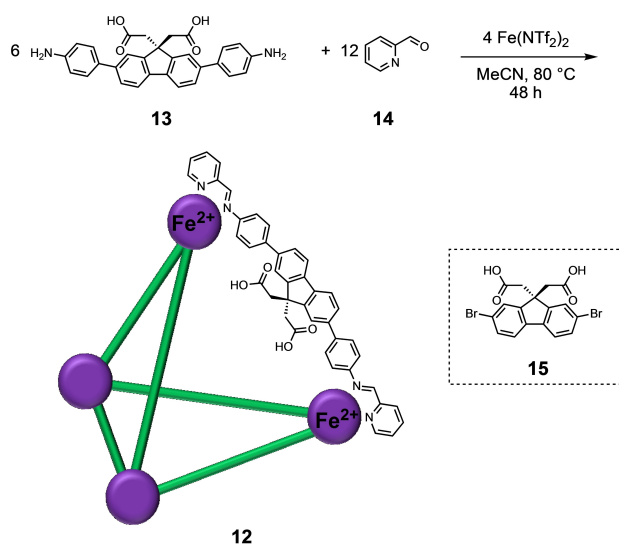


Figure 5. Synthesis of the *endo*-functionalized cage **12**. In the box is the acid-functionalized control compound **15** that is used for comparison.^[40]

endo-functionalization is needed for catalysis, as a $M_4L_6^{8+}$ cage-derivative of **12** that is not *endo*-functionalized, caused no aldehyde formation. **12** is also able to catalyze substitution

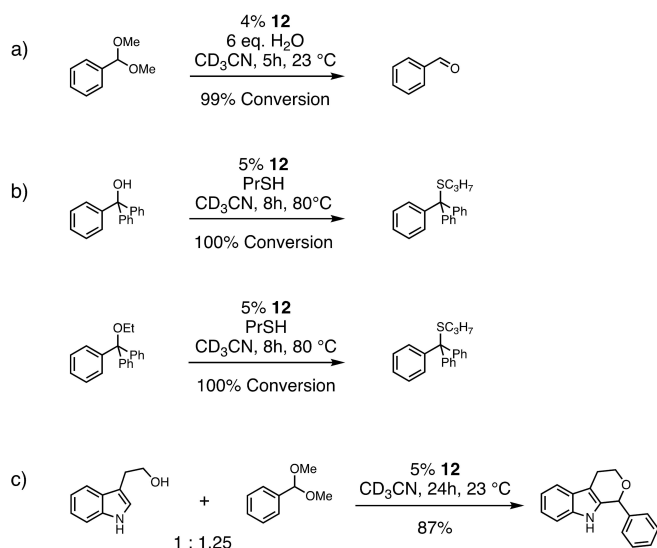


Figure 6. **12** as catalyst for the transformation of organic substrates: a) acetal hydrolysis;^[40] b) nucleophilic substitution;^[41] c) oxa-Pictet–Spengler reaction.^[42]

reactions of activated electrophiles like triphenylmethanol or its ethyl ether with thiols as nucleophiles (Figure 6b).^[41] Control acid **15** is again a way worse catalyst for this transformation as **12** operates with an acceleration of around 1000-fold compared to **15**. Also, amines like *N*-trityl-4-bromo-phenylaniline can be used as electrophile. However, in this case the liberated aniline reacts with the cage as it competes with **13** for the aldehyde **14**. This results in a destruction of the cage and hence a drop in catalytic performance, highlighting the role of **12** for the substitution reactions.

In a following study, Hooley reported on **12** as a catalyst for the oxa-Pictet–Spengler reaction.^[42] This cyclization between tryptophols and aldehyde derivatives is usually catalyzed by strong Lewis-acids such as AlCl_3 . While **12** is able to catalyze the reaction between tryptophols and acetals (Figure 6c) the unfunctionalized M_4L_6 cage-derivative and **15** are both not able to do so. Interestingly, the size of the acetals that can be converted is limited, as bulky ones such as 9-(dimethoxymethyl)anthracene give way lower yields. In addition to the reactions depicted in figure 6, cage **12** has been shown to catalyze the thioether/ether exchange in acetals and the thioetherification of tertiary allylic alcohols.^[43]

Derivatives of building block **13** have been synthesized as well. An example is the diamine functionalized building block **16** that assembles in the presence of 2-formylpyridine (**14**) and $\text{Fe}(\text{ClO}_4)_2$ to cage **17** (Figure 7).^[44] While the cage **17** is built from four iron ions, an excess iron salt was actually needed for the synthesis. ESI-MS of **17** revealed that 3–8 molecules HClO_4 are accompanying the cage. The HClO_4 may cause protonation of the NMe_2 groups, which is supported by broad peaks for these groups in the proton NMR. The origin of these protons is believed to be water formed upon the imine condensation that occurs during cage formation. The resulting hydroxide ions may react with residual iron which explains why an excess iron is

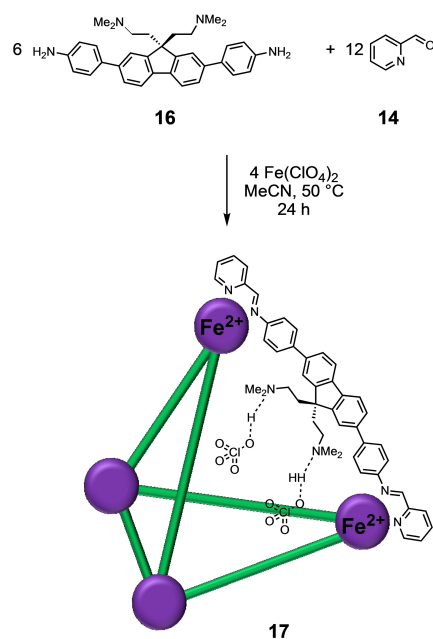


Figure 7. Synthesis of the *endo*-functionalized cage **17**.^[44]

needed for the synthesis of **17**. The deprotonation of the amines can be accomplished via an addition of an excess organic base such as DABCO. **17** is able to hydrolyze the acetal $\text{PhCH}(\text{OMe})_2$ in the presence of water and promotes amine detriylation. In a very recent work, a new generation of such M_4L_6 cages have been introduced. There the 2,7-diarylfluorene scaffold used for **12** and **17** has been changed for a 2,7-diarylcarbazole scaffold.^[45] As a consequence, now one instead of previous two *endo*-groups are employed per cage edge. New cages introduced in this work possess $\text{CH}_2\text{CH}_2\text{NMe}_2$ and $\text{CH}_2\text{CH}_2\text{SMe}$ functions as *endo*-groups.

The cages shown so far have been obtained via metal-ligand self-assembly. Endohedral-Functionalized cage compounds can also be of a purely organic nature. A particular interest in *endo*-functionalization lies in the modification of the *endo*-groups after sphere synthesis. The imine condensation reaction of triamine **18** with salicylaldehyde **19** leads to the *endo*-functionalized [4+6] cage **20** in 68% yield (Figure 8).^[46] Mastalerz showed that the *endo*-positioned hydroxy groups in **20** can be further manipulated to give several ethers such as the methoxyether-functionalized cage **21**. **21** is obtained in 81% yield via reaction of **20** with methyl iodide using potassium carbonate as base. Notably, the direct synthesis of **21** from **18** and the methoxy ether derivative of **19** gives the desired product only in a low yield of 17%. In addition to the low yields, **21** is obtained in a mixture from where it cannot be isolated from by chromatographic methods. The approach demonstrated by Mastalerz is an elegant way to circumvent such synthetic problems. In addition, this approach has the potential to allow a quick access to families of *endo*-functionalized cage compounds in good yields.

Chen introduced the organic cage **22** that is formed from **23** via reductive amination, followed by the removal of the

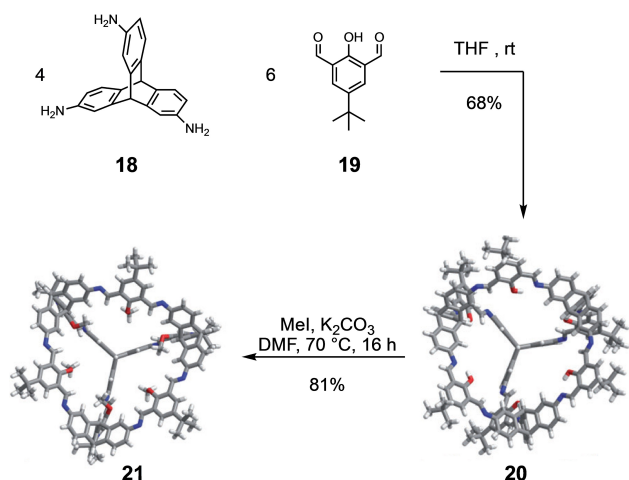


Figure 8. Synthesis of the purely organic *endo*-functionalized cage **20** and its post modification to **21**.^[46] **20** and **21** are depicted as their X-ray structures. Reproduced from Ref. [46] Copyright (2013), with permission from Wiley-VCH.

methoxymethyl (MOM) protection group and methylation of the secondary amines (Figure 9 top).^[47] Thus **22** is another example where functional group manipulation occurs after the cage has been synthesized. **22** possess endohedral hydroxy groups that are able to catalyze Friedel–Crafts allylations between *trans*- β -nitrostyrenes and 1-methylindole. For *trans*- β -nitrostyrene a yield of 86% was obtained with a cage-catalyst loading of 10% at room temperature and 168 h reaction time (Figure 9 bottom). Notably **22** performs significant better compared to uncaged model-compounds. Introducing two *tert*-

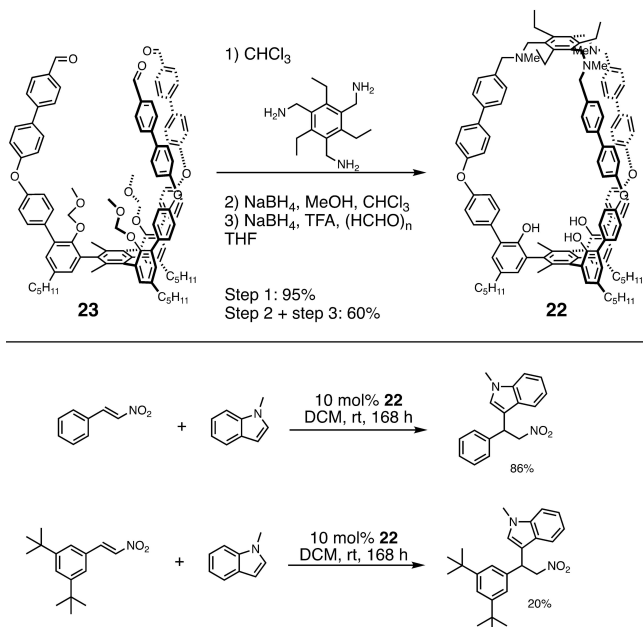


Figure 9. Synthesis of the purely organic *endo*-functionalized cage **22** and its application as a catalyst for the Friedel–Crafts reaction.^[47]

butyl-groups in meta position of the olefine substrate resulted in a low yield of 20%, indicating size-selectivity of **22** in this transformation.

Martinez and Dutasta presented the encaged Verkade's superbase **24** (Figure 10, left).^[48] This compound has been shown to be capable of catalyzing several reactions. As a base, **24** can catalyze Diels–Alder reactions.^[49] An example is the reaction between 3-hydroxy-2-pyrone and *N*-methylmaleimide (Figure 10, right). Interestingly, **24** can catalyze this reaction with a higher diastereoselectivity compared to a model compound that has no cage structure. This report is the first example of an encaged superbase as organocatalyst. In a later study, **24** has been shown to form a frustrated Lewis-pair (FLP) with TiCl_4 .^[50] The FLP is able to catalyze the Morita-Baylis-Hilman (MBH) reaction between *p*-chlorobenzaldehyde and cyclopent-2-en-1-one (Figure 10, right). While **24** gives a yield of 48% for this reaction, model-compounds that provide no cage structure gave the reaction product in smaller yield (17%) or not at all. This observation indicates that the reaction is occurring in the cavity. In an additional study by Martinez and Dufaud, protonated **24** and derivatives of it have been investigated for the ability to convert carbon dioxide with epoxides to cyclic carbonates.^[51] Within this study, it has been shown that caging of the active site protects it from deactivation pathways while increasing the catalytic activity for CO_2 conversion.

3. Endohedral Group Binds to a Functional Molecule

The introduction of endohedral groups in a cage can also be used to interact with guest molecules that are able to act as catalysts. Reek used this conceptual approach to design *endo*-guanidinium-binding site functionalized $\text{M}_{12}\text{L}_{24}$ Fujita-type spheres **25** (Figure 11a).^[52] The spheres assemble from building block **26** and Pd^{2+} or Pt^{2+} ions. The guanidinium-functionalization is able to interact with an encapsulated gold complex (TPPMSAu⁺; Figure 11b) via hydrogen bonding interaction between the guanidinium group and a sulfonate group located on the gold complex ligand. The binding of the sulfonate guests is strong ($> 10^5 \text{ M}^{-1}$ in CD_3CN). At the same time **25** is capable to host also carboxylate guests. These features have

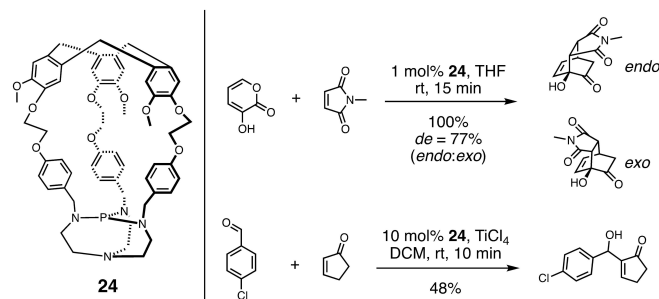


Figure 10. Encaged Verkade's superbase **24** and its application as catalyst for the Diels–Alder and Morita-Baylis-Hilman reactions.^[48–50]

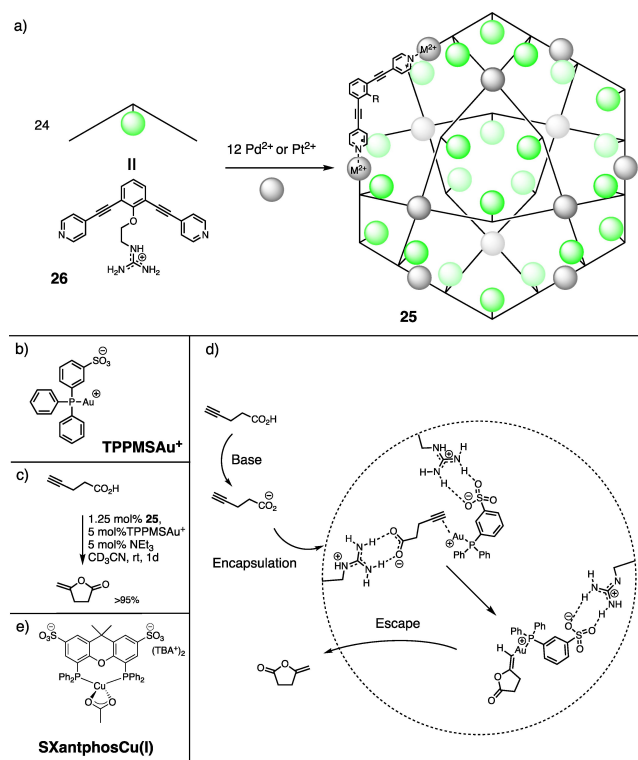


Figure 11. a) Synthesis of the *endo*-guanidinium-functionalized $M_{12}L_{24}$ spheres **25**; b) employed gold-catalyst TPPMSAu⁺; c) application of **25** in the gold-catalyzed cyclization of acetylenic acid; d) schematic representation how the sphere **25** enables the catalysis via preorganization of substrate and catalysts via hydrogen bonding interaction;^[52] e) employed copper-catalyst SXantphosCu(I).^[53]

been used to employ sphere **25** for the gold-catalyzed cyclization of 4-pentynoic acid (Figure 11c). Interestingly, the catalysis works best when the substrate is deprotonated (40 fold rate enhancement), while the conversion is way slower when base is absent and the substrate is present as an acid. This is explained via hydrogen bonding interactions between **25** and the catalyst and the carboxylate substrate at the same time. This results in a preorganization of both inside the sphere and hence a perfect match for catalysis (Figure 11d). The neutral enol lactone product can easily leave the cavity and cause no product inhibition as the carboxylate substrate is the preferred guest. The acid prior to deprotonation has only a little tendency to enter the sphere while the carboxylate binds with 10^3 M^{-1} in CD_3CN . This study presents a very interesting approach on how supramolecular catalysis might be selectively switched on and off.

Spheres **25** are able to host several equivalents of metal complexes at the same time. This results in a high local concentration of the catalyst, which is beneficial when the reaction requires for instance a bimetallic activation pathway of the substrate. The Cu(I)(Xantphos) catalyzed cyclization of 4-pentynoic acid to the corresponding enol lactone is such a reaction. Reek showed that a sulfonated analogue of XantphosCu(I), the so-called SXantphosCu(I) (Figure 11e), can be encapsulated in **25**.^[53] Overall, **25** can bind up to 12 equivalents

of copper catalyst. Interestingly, even when the average catalyst concentration is low, improved reaction rates are still observed with this system, showing the advantage of catalysis at high local concentrations.

The supramolecular binding of guests via an endohedral functionalization is an attractive alternative to employing this function directly via a covalent linker as endohedral group. It has been shown that this approach is also useful to host medicinal relevant compounds. Crowley demonstrated that Pd_2L_4 cages with $\text{L} = 2,6\text{-bis}(\text{pyridine-3-ylethynyl})\text{pyridine}$ are hosts of *cis*-platin.^[54] The binding occurs here via hydrogen bonding interactions between the amine ligands of platinum and the central pyridine moiety of the cage. Another advantage of this conceptual approach is that many different interior designs might be realized without synthesizing each time a new endohedral building block. However, differences in the reactivity between these two mentioned approaches, that is supramolecular via covalent functional group incorporation, have been observed. An example is the linker dependence for the electron transfer of redox-active species encapsulated in M_6L_{12} and $M_{12}L_{24}$ supramolecular cages.^[55]

4. Endohedral Group Acts as a Ligand

Endohedral groups can directly act as a ligand towards metals. Fujita reported an example, where the central arene in the bis(4-pyridyl)-functionalized building blocks, that are used to synthesize $M_{12}L_{24}$ spheres, was substituted for a pyridine.^[56] It has been shown that these pyridines could coordinate to transition metals. The pyridine functionalized $M_{12}L_{24}$ spheres have been reported to host 24 Ag^+ ions via pyridine coordination. Reek showed that via the use of Fujita type $M_{12}L_{24}$ spheres, catalysis at high local concentrations is possible. Two examples have already been discussed in the previous section where the *endo*-groups interacted with matching functionalized transition metal complexes. Prior to these studies, Reek demonstrated that $M_{12}L_{24}$ spheres can also be synthesized containing bis(4-pyridyl)-functionalized building blocks that have phosphine groups attached that coordinate already to gold (Figure 12). Combining these with ester *endo*-functionalized building blocks **28** results in the access of statistical mixtures of $M_{12}L_{24}$ spheres.^[57] Mixing **27** and **28** in ratios from 24:0 to 0:24

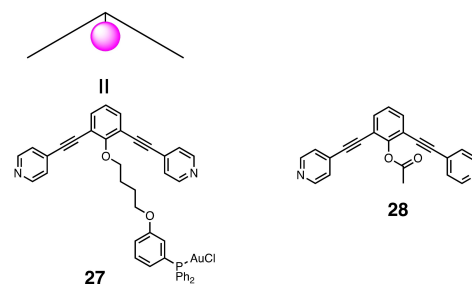
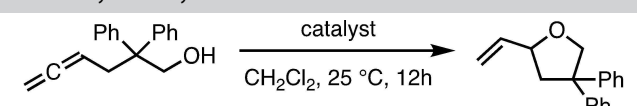


Figure 12. Building blocks **27** and **28** used to study the reactivity of statistical $M_{12}L_{24}$ sphere mixtures used in Table 1.^[57]

in the presence of Pd²⁺ ions created a series of statistical mixtures of M₁₂L₂₄ spheres possessing different average local concentrations of gold centers. However, the overall gold concentration is kept constant (except in the 0:24 case). This series of sphere mixtures has been investigated for the hydroalkoxylation of an allenol. A clear trend can be seen, which is that the yield increases with respect to increasing local gold concentrations (Table 1). Notably, the used AuCl complex is at low local concentration (1:23) inactive and gives hence no cyclization product. In a following study this approach was optimized by switching to Pt²⁺ based spheres, which resulted in more stable assemblies.^[58] These allow also the formation of

Table 1. Hydroalkoxylation of an allenol.^[57]



Entry	Ratio 27/28	Mol[%] spheres	Mol[%] 27	Yield [%]	TON
1	1:23	48	48	0	0
2	12:12	4	48	37	0.76
3	18:6	2.7	48	55	1.13
4	24:0	2	48	90	1.86

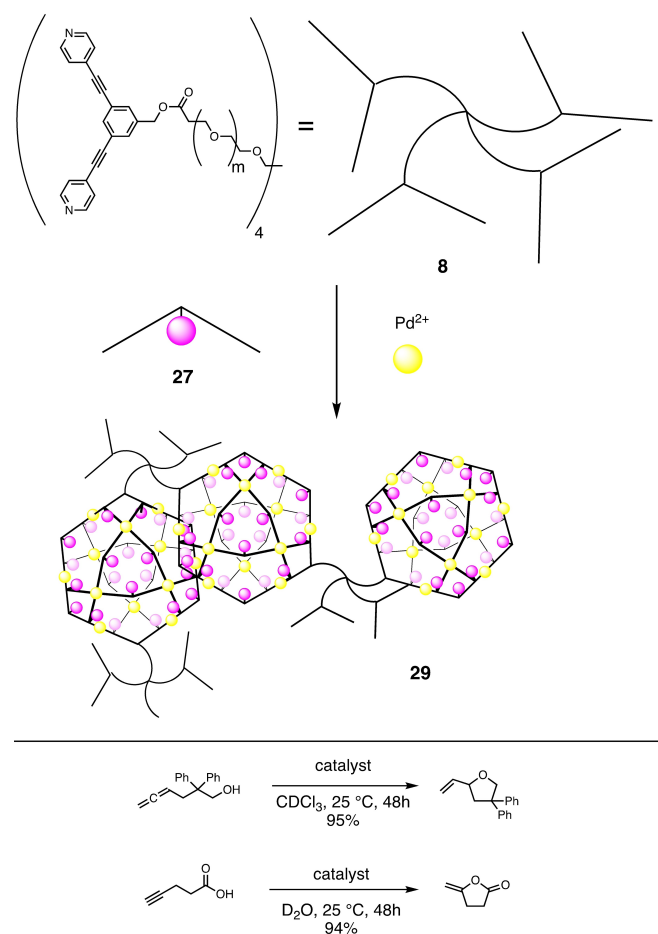


Figure 13. Top: Schematic depiction of the synthesis of M₁₂L₂₄²⁴⁺ sphere-based gels **29** via combination of **8** and **27**. Bottom: Application of M₁₂L₂₄²⁴⁺ sphere-based gels as catalysts for gold catalyzed cyclization reactions.^[39]

cationic gold complexes via the post sphere synthesis reaction with silver salts.

Oldenhuis and Johnson employed their approach to M₁₂L₂₄ sphere-based gels also to connected spheres that possess building block **27** (Figure 13).^[39] The gel **29** was used to study the cyclization of the allenol that was also explored by Reek. After a reaction time of 48 h, a conversion of 90% was reached. The activity of the gold-catalyst-functionalized gel was maintained for seven cycles. A conversion of 60% was still achieved after ten cycles and a TON of 41. Further, the cyclization of 4-pentynoic acid has been investigated. For this reaction the catalyst loses only very little activity over 12 recycling cycles. As an additional feature, catalysis in D₂O has been performed with the sphere containing gels.

The combination of bioinorganic chemistry with supramolecular cage compounds is a topic of growing interest.^[59] In recent years examples using *endo*-functional cage compounds emerged. Hydrogenases are metalloenzymes able to catalyze the reversible conversion of protons into molecular hydrogen at high rates and at almost no overpotential.^[60] For iron-iron hydrogenases it has been shown that one important feature is an internal proton relay.^[61] Inspired by these findings, Reek studied the mimicking of the iron-iron hydrogenase by using endohedral functionalized spheres.^[62] Within this report the authors mention that many synthetic analogous of this active site had been synthesized by that time but none where proton reduction would occur at a low overpotential. The approach chosen by Reek uses M₁₂L₂₄ spheres where two different ligands L are mixed in a 5:19 ratio. The ligand of which five equivalents have been used is the actual iron-iron hydrogenase active site mimic **30** (Figure 14). The other ligand

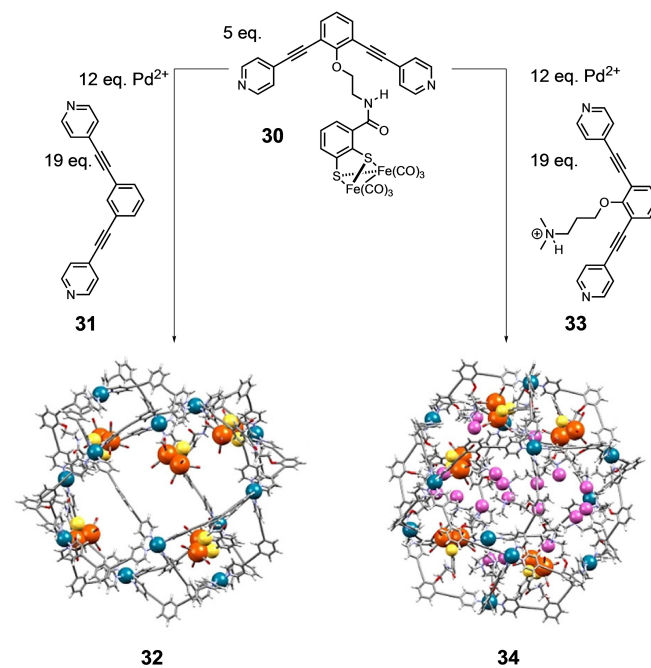


Figure 14. Synthesis of the spheres **32** and **34** that have been investigated as functional mimics of the iron-iron hydrogenase.^[62] Images of the molecular mechanics models are taken from reference 62.

31 is a bis(4-pyridyl)-functionalized building block that has no additional group for endohedral functionalization. Mixing these two building blocks with Pd²⁺ ions resulted in the formation of sphere **32**. Formation of the sphere resulted in a reduced overpotential for proton reduction of 230 mV compared to the free **30**. That is explained by the environment of the iron sites within the cage which results in stabilization of reduced reaction intermediates by the positive cage framework. Addition of an external acid is here necessary. Unfortunately, while the overpotential is reduced the catalytic rate is reduced as well. This observation has been addressed by changing **31** for building block **33** that possess an ammonium group capable of transferring protons and making the reaction faster. Mixing **30** and **33** resulted in the sphere **34** (Figure 14). Indeed, while a lowering of the overpotential was again observed (250 mV in comparison to **30**), the new sphere resulted in an enhancement of the reaction rate of more than two orders compared to **32**.

The metal coordination of three imidazole units belonging to histidine plays an important role in many metalloenzymes. For copper this is well known for several enzymes such as the Cu₆ site in particulate methane monooxygenase or tyrosinase.^[63–64] Otte mimicked such a coordination for copper containing enzymes via the use of the endohedral functionalized cage **36** (Figure 15).^[65] The cage is obtained via reductive amination of the triamine that was also used to synthesize **22** and the dialdehyde building block **35** that is already imidazole-functionalized. **36** is able to form complex **37** upon addition of copper(I) salts. The cage possesses a flexible structure due to the secondary amine groups that are next to two sp³ carbons. Within enzymes the coordinating groups are in close distance

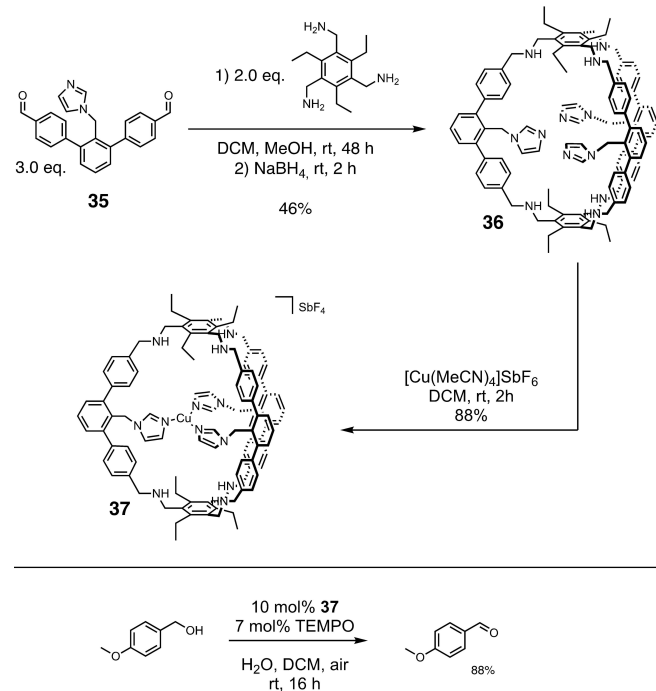


Figure 15. Synthesis of endohedral-functionalized cage **36** and its corresponding copper cage-complex **37**.^[65] Application of **37** as catalyst for the aerobic oxidation of alcohols.

while they can be on very different positions within the amino acid sequence. That behavior is somewhat mimicked in **37** as two coordinating nitrogen are 29 atoms apart. In the presence of TEMPO, cage-complex **37** is a catalyst for the aerobic oxidation of benzylic alcohols to benzyl aldehydes.

As the coordination spheres of many enzymatic active sites possess different types of amino acid ligands, it is of interest to employ this also in synthetic mimics. As many cage compounds assemble as the thermodynamic products in high symmetry it is challenging to synthesize cages of lower symmetry while maintaining the overall shape. For organic cages Otte reported on a stepwise approach using a derivative of the triamine used for the synthesis of **36** where one amine is masked via an azide. This approach can be used to synthesize organic cages with different endohedral groups and substitution patterns.^[66]

With this strategy, derivatives of **36** have been synthesized where one imidazole group has been substituted for a carboxylate group that is connected to the cage backbone via an alkyl linker. An example is the synthesis of **38**. Such a ligand sphere is used to mimic enzymatic iron active sites possessing the so-called 2histidine1carboxylate facial triad. This motif occurs in many non-heme iron enzymes such as naphthalene dioxygenase or taurine dioxygenase.^[67] For the synthesis of **38**, dialdehyde **35** reacts with the mentioned diamine **39** to give a macrocycle with azide groups (Figure 16).^[68] The azides can be transformed to amines via a Staudinger reaction resulting in macrocycle **40** which gives **38** after reaction with **41**. **38** is a

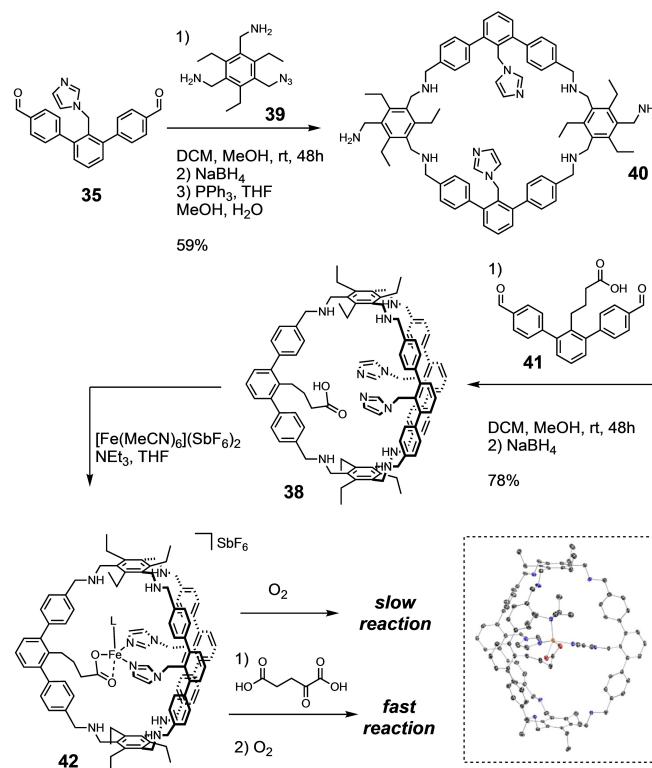


Figure 16. Synthesis of endohedral-functionalized cage **38** and its corresponding iron cage-complex **42**.^[68] Reactivity of **42** towards oxygen in absence and presence of alpha-ketoglutarate. Box shows the X-ray structure of the NEt₃ adduct of **42** taken from reference 68.

suitable ligand for transition metals. Within this study the coordination to zinc and iron has been investigated. Reaction of **38** with an iron salt results in the formation of a new species **42** that is paramagnetic. A synthetic challenge in the design of iron carboxyl complexes is to prevent the formation of carboxyl bridged dimeric species. DOSYNMR shows that no such dimerization occurs in solution for **42**. Further, the triethylamine adducts of **42** allowed to obtain a x-ray structure. That demonstrates that also in the solid state no dimerization occurs and that the ligand coordinates with both imidazoles and the carboxylate as a bidentate ligand, as it also occurs at the enzymatic active sites. In addition to the structural similarity, **42** mimics also the reactivity of such enzymes in a way that it does not react readily with oxygen. Many iron enzymes need co-substrates such as alpha-ketoglutarate to be able to activate oxygen. In the presence of alpha-ketoglutarate, **42** reacts directly with oxygen.

The particulate methane monooxygenase (pMMO) is an enzyme of very high interest. Its active site and its mechanism of action are under debate. In recent years the Cu_C site has been discussed to be the active site of pMMO.^[69–70] The ligand environment of the Cu_C site consists of two imidazoles and one carboxylate. Inspired by these results, Otte reported a derivative of **38** that has a shorter linker to the carboxylate group. That cage **43** has been shown to form the copper(I)-complex **44** (Figure 17).^[71] **44** can be chemically oxidized to the corresponding copper(II)-complex. This Cu(II) complex has in the presence of water EPR features that reveal strong similarities to the actual Cu_C site.^[69] **44** is able to oxidize hydroquinones to quinones under aerobic conditions. Such reactivity has been proposed to be important for methane oxidation by pMMO.^[70] Interestingly, empty cage **43** can perform also such oxidation but in lower yields compared to **44**. This may indicate a cooperative effect between the secondary amines and the copper center.

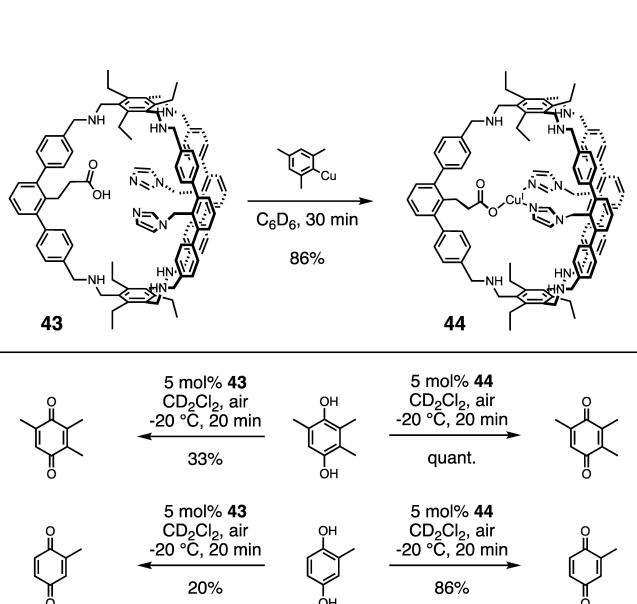


Figure 17. Synthesis of copper cage-complex **44** from **43** and the application of both for the aerobic oxidation of hydroquinones.^[71]

Hemicryptophanes have also been shown to use their amine functionalities to coordinate to transition metals. An example is **45**, which has been reported by Makita (Figure 18).^[72] **45** can be obtained from the corresponding empty hemicryptophane and $Zn(OAc)_2$. The cage-complex has been studied as a catalyst for the hydrolysis of *para*-nitrophenyl carbonate. This reaction results in the formation of the corresponding phenol, carbon dioxide and methanol. The performance of **45** has been compared with the uncapped **46**. Interestingly **45** is for the methyl carbonate 2.2 times faster compared to **46**. This ratio changes to 0.8 when the methyl group in the carbonate is changed for a *tert*-butyl group. One possible explanation could be that the enhanced size of the substrate hinders the ability to reach the catalytic active site within **45**.

Inspired by copper containing enzymes, Dutasta and Martinez used a hemicryptophan to study its binding to copper.^[73] The copper(II)-complex **47** was used to catalyze the oxidation of cyclohexane to cyclohexanol and cyclohexanone (Figure 19). At 35 °C and a catalyst loading of 1 mol% a yield of 28% oxidation products was obtained using 10 equivalents hydrogen peroxide as the oxidative reagent. The alcohol ketone ratio is under these conditions 4:3. The performance of **47** was compared with the uncapped catalyst **48**. Under the mentioned conditions, **48** gives a yield of 15% of oxidation products with an alcohol to ketone ratio of 2:1. Kinetic investigation shows that the conversion using **48** stops after 1 h while **47** stays another hour active, explaining the roughly 2-fold higher yield. It seems that the cage has an impact on the catalyst deactivation and prevents it at least for some time. Within this study, a size-dependence of substrates has also been investigated. In competition experiments between cyclohexane and adamantane, different conversion ratios have been observed for

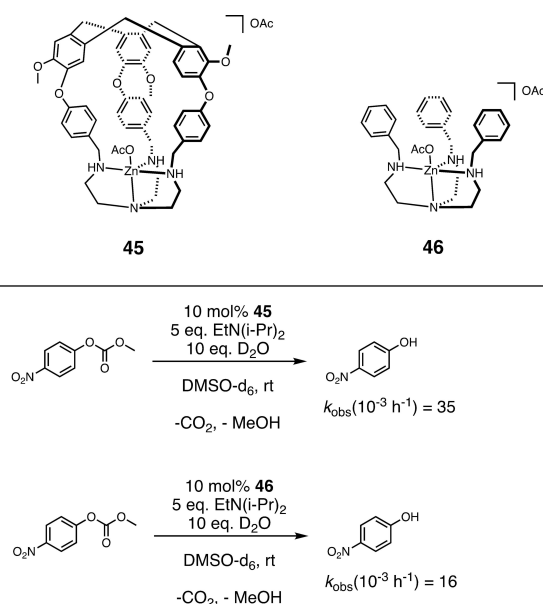


Figure 18. Hemicryptophane **45** and its use as catalyst for the hydrolysis of carbonates. Comparison to the uncapped **46**.^[72]

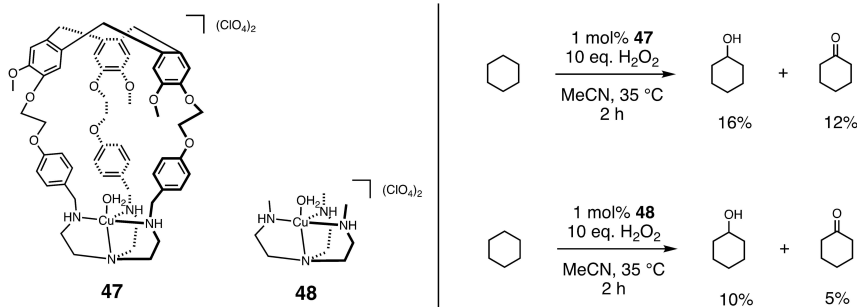


Figure 19. Hemicryptophan copper(II)-complex **47** and its use as catalyst for the oxidation of cyclohexane with comparison to model-complex **48**.^[73]

47 and **48**. While it is 5 for the cage-catalyst **47**, it is only 1.7 for the model complex **48**.

In a subsequent study, Guy, Gao and Martinez introduced a set of hemicryptophans that possesses binaphthol moieties.^[74] These compounds were used by Martinez to synthesize the oxido-vanadium(V)-complexes **49** (Figure 20).^[75] Further their uncapped derivatives **50** were synthesized to evaluate the cage effect. This work built also on a previous study by Dutasta where hemicryptophan oxido-vanadium(V)-complexes have been used to sulfoxidize thioanisol and other thioethers with turnover numbers (TONs) of up to 180.^[76] The aim behind these new ligands was to construct more hydrophobic cavities. Further, it should result in a better isolation of the reactive center from the bulk solution. With this new set of complexes, the catalytic sulfoxidation of thioanisol was investigated (Figure 20). Using cumene hydroperoxide (CHP) as oxidant and a catalyst loading of 1.5 mol% in DCM at 0 °C gave with **49** the oxidized product after 180 min with yields between 85 and 93%. The uncapped set of catalysts **50** gave yields between 15 and 16%, highlighting the advantage of the capped catalyst. Using *M*-(*S,S,S*)-(R,R,R)-**49**, at catalyst loadings of 0.01 mol% at room temperature resulted in a yield on 85% after 10 h. After 13 h, TONs of up to 10000 were reached. No loss in catalytic activity was found over four-cycle experiments. The catalytic

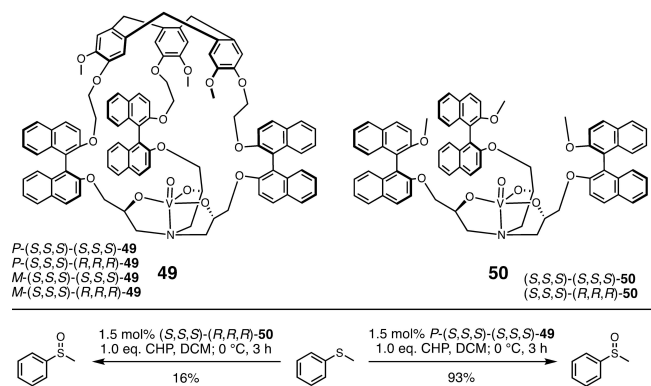


Figure 20. Hemicryptophan oxido-vanadium(V)-complex **49** and its use as catalyst for the sulfoxidation of thioanisol with comparison to model-complex **50**.^[75]

system follows Michaelis–Menten kinetics. Notably, catalyst performance can be inhibited when Me_4N^+ is added as a competitive guest.

Sorokin and Martinez used hemicryptophan metal-complexes to study their ability towards methane oxidation.^[77] Methane oxidation is difficult due to the high C–H bond dissociation energy of 104.9 kcal mol⁻¹. Further, it is very difficult to have a selective oxidation to methanol as this product is easier oxidized than methane, which results in over oxidation. Among the complexes investigated in the study by Sorokin and Martinez are **47** and **49** but also derivatives that offer a tris(2-pyridylmethyl)amine-based (TPA) ligand sphere. These are the copper(II)- and iron(II)-complexes **51** and **52** (Figure 21). The complexes tested are inspired by the pMMO where the active site is presumably in a hydrophobic cavity which should be mimicked by the cage. Reaction conditions employed use the cage catalyst in the presence of methane (30 bar) in water at 60 °C and hydrogen peroxide as the solvent. The presence of formic acid, formaldehyde, methyl hydroperoxide and methanol as reaction products was analyzed (Table 2). The copper complexes **47**, **48** and **51** show only low total TONs for methane with **47** having the highest with 1.8. **47** is also the only copper complex in this study where methanol formation was observed (TON 0.3). The vanadium-complexes give the highest TONs in this study. **49** is here shown as an example with a total TON of 13.2. Most of the formed product is formic acid with 10.1 while methanol is formed with a TON of

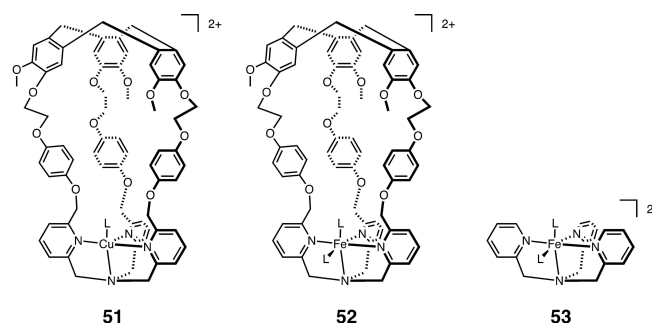


Figure 21. Hemicryptophan-complexes **51** and **52** that contain a TPA motive and its uncapped iron-complex **53**. These were used to study the oxidation of methane.^[77]

Table 2. Methane oxidation catalyzed by hemicyptophan-complexes and comparison to their uncaged model compounds.^[77]

Catalyst	CH ₄ (30 bar)				Total TON
	HCOOH TON	HCHO TON	CH ₃ OOH TON	CH ₃ OH TON	
47	1.3	0.2	none	0.3	1.8
48	0.5	none	0.1	none	0.6
51	1.4	0.1	none	none	1.5
49	10.1	2.4	none	0.7	13.2
52	4.7	2.0	1.4	1.1	9.2
53	1.7	2.3	0.7	none	4.7

Reaction conditions: CH₄ (30 bar) + H₂O₂ (0.33 M) with catalyst (1 μmol) in H₂O at 60 °C for 20 h. Products: HCOOH + HCOH + CH₃OOH + CH₃OH.

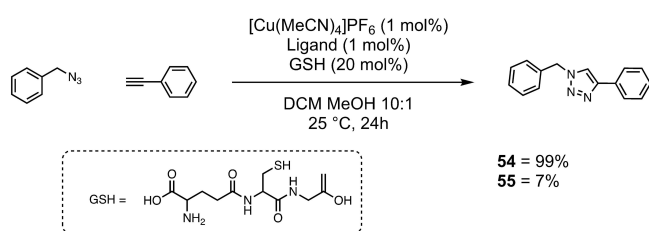
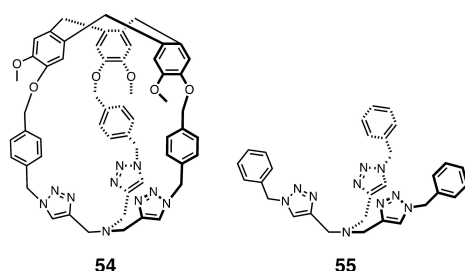


Figure 22. TBTA-functionalized hemicyptophan **54** and its model **55** that have been used to study the CuAAC in the presence of its inhibitor GSH.^[79]

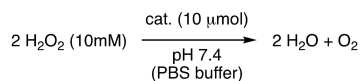
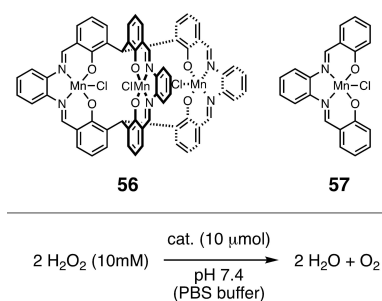


Figure 23. Tri-Mn(Salen) cryptand **56** that has been investigated on its ability to transform hydrogenperoxide into oxygen and water.^[80]

0.7. The iron(II)-complexes **52** and **53** give total TONs of 9.2 and 4.7. As for the other systems in table 2, formic acid is for both complexes the major product formed. However, **52** forms methanol with a TON of 1.1, which is the highest observed in this study.

The tris(benzyltriazolemethyl)-amine (TBTA) motive has also been incorporated in organic cage type compounds. David

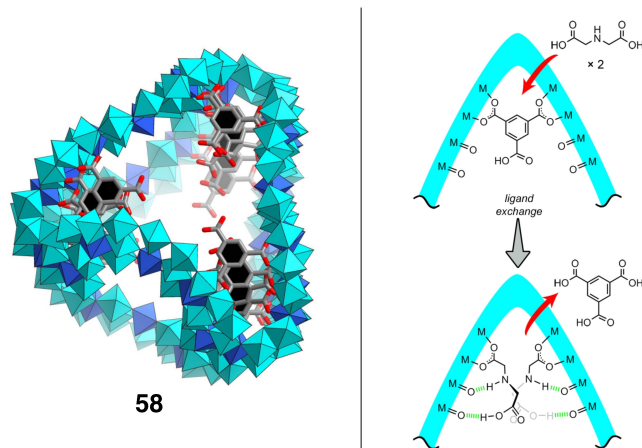


Figure 24. X-ray structure of **58** and schematic representation of the substitution reaction of 1,3,5-benzenetricarboxylate for iminodiacetic acid.^[103] Reproduced from Ref. [103] Copyright (2022), with permission from Wiley-VCH.

reported the coordination to zinc by such systems.^[78] In a recent study, Martinez and Colomban incorporated the TBTA motive in a hemicyptophan.^[79] The resulting ligand **54** is capable to catalyze the Cu-catalyzed azide-alkyne cycloaddition (CuAAC) (Figure 22). The results were compared with the uncaged model ligand **55**. Interestingly, in most cases the uncaged system performed better. However, when the click reaction was performed in the presence of the biological CuAAC inhibitor glutathione (GSH), superior yields have been obtained with **54**, while **55** performs only poorly. These results indicate that **54** is capable to protect the active copper site from inhibitor.

Inspired by the antioxidant properties of natural catalases, Kang, Sessler and Zhang reported on tri-Mn(Salen) cryptands. The aim of these cryptands is to act as potential antioxidant metallodrugs.^[80] The cryptands have been investigated for their ability to transform hydrogen peroxide into oxygen and water. An example of the tested compounds is cage-complex **56** (Figure 23). In comparison to control complex **57**, **56** produces dioxygen 6.8 times faster. The reaction occurs in PBS buffer at a pH of 7.4. In a following work, **56** has been combined with a photosensitizer to construct a programmable phototheranostics.^[81]

5. Conclusion and Outlook

Endohedral-functionalized cage compounds are a research field of growing interest. Within this article the application of such cages for their ability to mediate or catalyze reactions within their cavities has been reviewed. In addition to this aspect, other applications of endohedral-functionalized cage compounds have been explored and for some of these it is likely that they will contribute at some time to catalysis inside cavities.

One current aspect in cage chemistry is the development of systems that have the ability to switch a certain behavior on demand on and off. Fujita reported on $M_{12}L_{24}$ spheres that have due to endohedral-functionalization 24 azobenzene moieties in their cavity. Upon photoisomerization the hydrophobic environment in the sphere can be fine-tuned and hence the guest uptake can be controlled.^[82] Molecular motors are a field of very high importance that is related to supramolecular chemistry.^[83] Molecular rotors as such introduced by Feringa have been of particular interest in the last decades.^[84] Clever installed molecular rotors as endohedral-functionalization in Pd_2L_4 cages.^[85] The dynamics of the reported push-pull rotors is among other factors influenced by the derivatization of the electron-withdrawing moieties. Li, Zhang and Zheng introduced recently Pd_2L_4 cages that have endohedral groups that possess a light-triggered rotary function and be able to host C_{60} as a guest.^[86]

Within cage chemistry, it is often mentioned that enzymes are a major inspiration. As also discussed in this manuscript, mimicking the enzymatic active sites while mimicking the active site pocket via cage compounds at the same time leads to new pathways in bioinorganic chemistry. Another approach is to use cages as hosts for enzymes. Fujita reported in 2007 a first step in this direction when $M_{12}L_{24}$ spheres have been reported that offer peptides as endohedral-functionalization.^[87] In 2012, Kato and Fujita showed that $M_{12}L_{24}$ spheres can also host a protein.^[88] The sphere was assembled via reaction of 23 equivalents of unfunctionalized bis(4-pyridyl) building block and one equivalent of protein functionalized building block in the presence of Pd^{2+} ions. The protein is anchored via reaction of a cysteine thiol group with the maleimide of the functionalized building block. Fujita and Fujita showed 2021 that encapsulation of a cutinase-like enzyme in a molecular cage can stabilize its tertiary structure.^[89] It has further been demonstrated that this improves the enzymatic activity. When the confined enzyme was exposed to an organic solvent, like acetonitrile, its half-life was prolonged 1000-fold.

The formation of a cage-compound can be controlled via *endo*-functionalization. Beuerle studied the reaction of hexahydroxy tribenzotriquinacene with meta terphenyl-based diboronic acid compounds.^[90] The unsubstituted 120° bite angle compound assembles to a [4+6] cage compound. Upon introduction of an additional benzoic acid substituent at the 2'-position of the terphenyl-based diboronic acid compound a [2+3] cage is observed as the major product. The new selectivity is explained via hydrogen bonding interactions of the endohedral boronic acid groups, which overcompensate the strain of the smaller cage. A study of Reek showed, that for the selective formation of Fujita-type $Pt_{12}L_{24}$ spheres, functionalization of the ligands plays a role.^[91]

Endohedral-functionalization can also be combined with other supramolecular motifs. Stoddart and Fujita showed that $M_{12}L_{24}$ spheres can be equipped with pseudo-rotaxane groups.^[92] These are based on a tetracationic cyclophane host, cyclobis(paraquat-*p*-phenylene), and a 1,5-dioxynaphthalene guest. This system showed a stimulus-responsive behavior towards ions. Furthermore, as the cyclophane host is 4⁺

charged this system is an example of encapsulated cations inside cations. Liu showed that crown ether moieties can be incorporated in Pd_6L_{12} cages.^[93] These can host potassium cations which allows inclusion of boron-dipyrromethene dyes into the cage cavities. These host-guest complexes display a circularly polarized luminescence, while both cage and dye by themselves do not show such behavior.

Hosting of oxo-anions by cage compounds is for environmental reasons of interest as such host-guest interactions might be used to purify contaminated industrial water.^[94] Also for medicinal reasons, such host-guest complexes can be of interest. Archibald and Lusby reported the encapsulation of TcO_4^- and ReO_4^- (often used as TcO_4^- -surrogate) in a cobalt-coordination cage.^[95] TcO_4^- is used in clinical nuclear diagnostic imaging scans. The reported TcO_4^- cage host-guest complex showed a different biodistribution compared to the free oxo-anion. Pasini and Amendola employed a chiral cage as a chiroptical sensor for ReO_4^- in aqueous media.^[96] The used cryptand is of low symmetry and contains a 1,1'-binaphthyl-2,2'-diol (BINOL) moiety as endohedral-functionalization. The synthesis occurs via a reductive amination protocol from a diamine-functionalized macrocycle and 2,2'-dihydroxy-1,1'-binaphthyl-3,3'-dicarbaldehyde. These systems present another example of the successful combination of low-symmetry cages and endohedral-functionalization.

Endohedral-functionalized cages of lower-symmetry, which assemble via metal ligand coordination have been shown to be suitable for binding guests. Clever introduced such heteroleptic $[Pd_2L^1L^2L^3]$ cages via a shape complementary assembly. That is that the bite angles of the ligands used direct the cage formation. These cages possess endohedral carbazole motifs that are either N-H or otherwise functionalized, such as N- CH_3 .^[97] These compounds have been studied for their ability to bind to deprotonated phosphate diesters. A system with a N-H group shows significant higher binding constants in comparison to its N- CH_3 derivative, which is explained via the possibility to form hydrogen bonds. Very recently, Clever demonstrated the synthesis of a $[Pd_2L^1L^2L^3L^4]$ cage by a combination of ligand shape complementary, strain balance and inter ligand C-H- π interaction.^[98] In addition to the bite angle control of the building blocks, heteroleptic cages have also been shown to be synthesized via ligand interaction such as steric bulk or hydrogen bonding interactions.^[99,100] Zhang used such an approach to design endohedral-functionalized $[Pd_2L^1L^2L^3L^4]$ cages.^[101] The synthesis of these cages starts with the formation of a $[Pd_2L^1L^2]$ macrocyclic species. The ligands are here *trans* to each other. Methyl-functionalization of the coordinating pyridines avoids here the formation of an undesired cage. The $[Pd_2L^1L^2]$ macrocyclic species is reacted with L^2 leading to a bowl type species $[Pd_2L^1L^2L^2]$. L^2 introduces an *endo*-functionalization to the bowl. This functionalization is sterically demanding and hence does not allow the formation of a $[Pd_2L^1L^2L^2]$ cage. The bowl reacts afterwards with L^3 to the desired $[Pd_2L^1L^2L^2L^3]$ cages. Ligand L^3 can introduce a second, but sterically less demanding endohedral-functionalization to the cage.

It has also been shown that endohedral-functionalization can be introduced after the cage has been formed. Hooley reported that smaller derivatives of **17** that possess no *endo*-functionalization can undergo iron-catalyzed C–H oxidation on the fluorene moieties. The hydroxylation occurring is diastereoselective in the presence of templating counter ions that are encapsulated in the cage.^[102] Very recently, Fang demonstrated that *endo*-functionalization can be exchanged after the cage has been assembled.^[103] The polyoxometalate cages **58** studied can host aromatic carboxylates such as 1,3,5-benzenetricarboxylate (Figure 24, left). These aromatic carboxylates can be substituted for others such as iminodiacetic acid (Figure 24, right).

In conclusion, the field of endohedral cages is vibrant and many recent findings promise more spectacular results to come in the next years. In particular, it will be interesting to see the application of such cages that combine this approach with other approaches mentioned in figure 1 or additional approaches in cage chemistry that may develop over time.

Acknowledgements

Emily C. Monkcom is thanked for the work on the cover feature. Open Access funding enabled and organized by Projekt DEAL.

Conflict of Interest

The authors declare no conflict of interest.

Keywords: bioinorganic chemistry · confined space · organocatalysis · self-assembly · size-selective catalysis

- [1] M. Yoshizawa, M. Tamura, M. Fujita, *Science* **2006**, *312*, 251–254.
- [2] Q. Shi, D. Masseroni, J. Rebek, *J. Am. Chem. Soc.* **2016**, *138*, 10846–10848.
- [3] M. D. Pluth, R. G. Bergman, K. N. Raymond, *Science* **2007**, *316*, 85–88.
- [4] Q. Zhang, K. Tiefenbacher, *J. Am. Chem. Soc.* **2013**, *135*, 16213–16219.
- [5] T. A. Bender, R. G. Bergman, K. N. Raymond, F. D. Toste, *J. Am. Chem. Soc.* **2019**, *141*, 11806–11810.
- [6] M. L. Merlau, M. del Pilar Mejia, S. B. T. Nguyen, J. T. Hupp, *Angew. Chem. Int. Ed.* **2001**, *40*, 4239–4242; *Angew. Chem.* **2001**, *113*, 4369–4372.
- [7] a) M. Otte, P. F. Kuijpers, O. Troepfner, I. Ivanović-Burmazović, J. N. H. Reek, B. de Bruin, *Chem. Eur. J.* **2013**, *19*, 10170–10178; b) P. F. Kuijpers, M. Otte, M. Dürr, I. Ivanović-Burmazović, J. N. H. Reek, B. de Bruin, *ACS Catal.* **2016**, *6*, 3106–3112.
- [8] W. Meng, B. Breiner, K. Rissanen, J. D. Thoburn, J. K. Clegg, J. R. Nitschke, *Angew. Chem. Int. Ed.* **2011**, *50*, 3479–3483; *Angew. Chem.* **2011**, *123*, 3541–3545.
- [9] D. H. Leung, R. G. Bergman, K. N. Raymond, *J. Am. Chem. Soc.* **2007**, *129*, 2746–2747.
- [10] C. J. Brown, F. D. Toste, R. G. Bergman, K. N. Raymond, *Chem. Rev.* **2015**, *115*, 3012–3035.
- [11] M. M. Conn, J. Rebek, *Chem. Rev.* **1997**, *97*, 1647–1668.
- [12] G. Zhang, M. Mastalerz, *Chem. Soc. Rev.* **2014**, *43*, 1934–1947.
- [13] A. Schmidt, V. Molano, M. Hollering, A. Pöthig, A. Casini, F. E. Kühn, *Chem. Eur. J.* **2016**, *22*, 2253–2256.
- [14] K. Wu, B. Zhang, C. Drechsler, J. J. Holstein, G. H. Clever, *Angew. Chem. Int. Ed.* **2021**, *60*, 6403–6407; *Angew. Chem.* **2021**, *133*, 6473–6478.
- [15] Q.-F. Sun, T. Murase, S. Sato, M. Fujita, *Angew. Chem. Int. Ed.* **2011**, *50*, 10318–10321; *Angew. Chem.* **2011**, *123*, 10502–10505.
- [16] M. L. Schneider, J. A. Campbell, A. D. Slattey, W. M. Bloch, *Chem. Commun.* **2022**, *58*, 12122–12125.
- [17] J.-X. Ma, J. Li, Y.-F. Chen, R. Ning, Y.-F. Ao, J.-M. Liu, J. Sun, D.-X. Wang, Q.-Q. Wang, *J. Am. Chem. Soc.* **2019**, *141*, 3843–3848.
- [18] Q. Zhu, X. Wang, R. Clowes, P. Cui, L. Chen, M. A. Little, A. I. Cooper, *J. Am. Chem. Soc.* **2020**, *142*, 16842–16848.
- [19] R. L. Greenaway, V. Santolini, F. T. Szczypiński, M. J. Bennison, M. A. Little, A. Marsh, K. E. Jelfs, A. I. Cooper, *Chem. Eur. J.* **2020**, *26*, 3718–3722.
- [20] F. Dournel, M. Koshan, P. Woite, M. Roemelt, M. Otte, *RSC Adv.* **2022**, *12*, 3402–3405.
- [21] D. Samanta, P. S. Mukherjee, *Chem. Commun.* **2013**, *49*, 4307–4309.
- [22] W. M. Bloch, J. J. Holstein, W. Hiller, G. H. Clever, *Angew. Chem. Int. Ed.* **2017**, *56*, 8285–8289; *Angew. Chem.* **2017**, *129*, 8399–8404.
- [23] R.-J. Li, A. Tarzia, V. Posligua, K. E. Jelfs, N. Sanchez, A. Marcus, A. Baksi, G. H. Clever, F. Fadaei-Tirani, K. Severin, *Chem. Sci.* **2022**, *13*, 11912–11917.
- [24] S. Klotzbach, F. Beuerle, *Angew. Chem. Int. Ed.* **2015**, *54*, 10356–10360; *Angew. Chem.* **2015**, *127*, 10497–10502.
- [25] a) D. Beaudoin, F. Rominger, M. Mastalerz, *Angew. Chem. Int. Ed.* **2017**, *56*, 1244–1248; *Angew. Chem.* **2017**, *129*, 1264–1268; b) P. Wagner, F. Rominger, W.-S. Zhang, J. H. Gross, S. M. Elbert, R. R. Schröder, M. Mastalerz, *Angew. Chem. Int. Ed.* **2021**, *60*, 8896–8904; *Angew. Chem.* **2021**, *133*, 8978–8986.
- [26] V. Croué, S. Goeb, G. Szalóki, M. Allain, M. Sallé, *Angew. Chem. Int. Ed.* **2016**, *55*, 1746–1750; *Angew. Chem.* **2016**, *128*, 1778–1782.
- [27] C. S. Wood, C. Browne, D. M. Wood, J. R. Nitschke, *ACS Cent. Sci.* **2015**, *1*, 504–509.
- [28] H. Lee, J. Tessarolo, D. Langbehn, A. Baksi, R. Herges, G. H. Clever, *J. Am. Chem. Soc.* **2022**, *144*, 3099–3105.
- [29] E. Nieland, J. Voss, A. Mix, B. M. Schmidt, *Angew. Chem. Int. Ed.* **2022**, *61*, e202212745; *Angew. Chem.* **2022**, *134*, e202212745.
- [30] R. G. DiNardi, A. O. Douglas, R. Tian, J. R. Price, M. Tajik, W. A. Donald, J. E. Beves, *Angew. Chem. Int. Ed.* **2022**, *61*, e202205701; *Angew. Chem.* **2022**, *134*, e202205701.
- [31] D. Hugenbusch, M. Lehr, J.-S. von Glasenapp, A. J. McConnell, R. Herges, *Angew. Chem. Int. Ed.* **2023**, *62*, e202212571; *Angew. Chem.* **2023**, *135*, e202212571.
- [32] P. M. Bogie, T. F. Miller, R. J. Hooley, *Isr. J. Chem.* **2019**, *59*, 130–139.
- [33] M. Tominaga, K. Suzuki, T. Murase, M. Fujita, *J. Am. Chem. Soc.* **2005**, *127*, 11950–11951.
- [34] T. Murase, S. Sato, M. Fujita, *Angew. Chem. Int. Ed.* **2007**, *46*, 1083–1085; *Angew. Chem.* **2007**, *119*, 1101–1103.
- [35] K. Suzuki, S. Sato, M. Fujita, *Nat. Chem.* **2010**, *2*, 25–29.
- [36] Y. Ueda, H. Ito, D. Fujita, M. Fujita, *J. Am. Chem. Soc.* **2017**, *139*, 6090–6093.
- [37] S. B. Jones, B. Simmons, A. Mastracchio, D. W. C. MacMillan, *Nature* **2011**, *475*, 183–188.
- [38] X. Yan, P. Wei, Y. Liu, M. Wang, C. Chen, J. Zhao, G. Li, M. L. Saha, Z. Zhou, Z. An, X. Li, P. J. Stang, *J. Am. Chem. Soc.* **2019**, *141*, 9673–9679.
- [39] C. M. Brown, D. J. Lundberg, J. R. Lamb, I. Kevlishvili, D. Kleinschmidt, Y. S. Alfaraj, H. J. Kulik, M. F. Ottaviani, N. J. Oldenhuis, J. A. Johnson, *J. Am. Chem. Soc.* **2022**, *144*, 13276–13284.
- [40] L. R. Holloway, P. M. Bogie, Y. Lyon, C. Ngai, T. F. Miller, R. R. Julian, R. J. Hooley, *J. Am. Chem. Soc.* **2018**, *140*, 8078–8081.
- [41] P. M. Bogie, L. R. Holloway, C. Ngai, T. F. Miller, D. K. Grewal, R. J. Hooley, *Chem. Eur. J.* **2019**, *25*, 10232–10238.
- [42] C. Ngai, C. M. Sanchez-Marsetti, W. H. Harman, R. J. Hooley, *Angew. Chem. Int. Ed.* **2020**, *59*, 23505–23509; *Angew. Chem.* **2020**, *132*, 23711–23715.
- [43] C. Ngai, B. da Camara, C. Z. Woods, R. J. Hooley, *J. Org. Chem.* **2021**, *86*, 12862–12871.
- [44] C. Ngai, H.-T. Wu, B. da Camara, C. G. Williams, L. J. Mueller, R. R. Julian, R. J. Hooley, *Angew. Chem. Int. Ed.* **2022**, *61*, e202117011; *Angew. Chem.* **2022**, *134*, e202117011.
- [45] C. Z. Woods, H.-T. Wu, C. Ngai, B. da Camara, R. R. Julian, R. J. Hooley, *Dalton Trans.* **2022**, *51*, 10920–10929.
- [46] M. W. Schneider, I. M. Oppel, A. Griffin, M. Mastalerz, *Angew. Chem. Int. Ed.* **2013**, *52*, 3611–3615; *Angew. Chem.* **2013**, *125*, 3699–3703.
- [47] H.-Y. Chen, M. Gou, J.-B. Wang, *Chem. Commun.* **2017**, *53*, 3524–3526.
- [48] P. D. Raytchev, A. Martinez, H. Gornitzka, J.-P. Dutasta, *J. Am. Chem. Soc.* **2011**, *133*, 2157–2159.

- [49] B. Chatelet, V. Dufaud, J.-P. Dutasta, A. Martinez, *J. Org. Chem.* **2014**, *79*, 8684–8688.
- [50] J. Yang, B. Chatelet, V. Dufaud, D. Héroult, S. Michaud-Chevallier, V. Robert, J.-P. Dutasta, A. Martinez, *Angew. Chem. Int. Ed.* **2018**, *57*, 14212–14215; *Angew. Chem.* **2018**, *130*, 14408–14411.
- [51] B. Chatelet, L. Joucla, J.-P. Dutasta, A. Martinez, V. Dufaud, *Chem. Eur. J.* **2014**, *20*, 8571–8574.
- [52] Q.-Q. Wang, S. Gonell, S. H. A. M. Leenders, M. Dürr, I. Ivanović-Burmazović, J. N. H. Reek, *Nat. Chem.* **2016**, *8*, 225–230.
- [53] S. Gonell, X. Caumes, N. Orth, I. Ivanović-Burmazović, J. N. H. Reek, *Chem. Sci.* **2019**, *10*, 1316–1321.
- [54] J. E. M. Lewis, E. L. Gavey, S. A. Cameron, J. D. Crowley, *Chem. Sci.* **2012**, *3*, 778–784.
- [55] R. Zaffaroni, E. O. Bobylev, R. Plessius, J. I. van der Lugt, J. N. H. Reek, *J. Am. Chem. Soc.* **2020**, *142*, 8837–8847.
- [56] K. Harris, Q.-F. Sun, S. Sato, M. Fujita, *J. Am. Chem. Soc.* **2013**, *135*, 12497–12499.
- [57] R. Gramage-Doria, J. Hessels, S. H. A. M. Leenders, O. Tröppner, M. Dürr, I. Ivanović-Burmazović, J. N. H. Reek, *Angew. Chem. Int. Ed.* **2014**, *53*, 13380–13384; *Angew. Chem.* **2014**, *126*, 13598–13602.
- [58] S. H. A. M. Leenders, M. Dürr, I. Ivanović-Burmazović, J. N. H. Reek, *Adv. Synth. Catal.* **2016**, *358*, 1509–1518.
- [59] J.-N. Rebilly, B. Colasson, O. Bistri, D. Over, O. Renaud, *Chem. Soc. Rev.* **2015**, *44*, 467–489.
- [60] W. Lubitz, H. Ogata, O. Rüdiger, E. Reijerse, *Chem. Rev.* **2014**, *114*, 4081–4148.
- [61] C. Sommer, A. Adamska-Venkatesh, K. Pawlak, J. A. Birrell, O. Rüdiger, E. J. Reijerse, W. Lubitz, *J. Am. Chem. Soc.* **2017**, *139*, 1440–1443.
- [62] R. Zaffaroni, N. Orth, I. Ivanović-Burmazović, J. N. H. Reek, *Angew. Chem. Int. Ed.* **2020**, *59*, 18485–18489; *Angew. Chem.* **2020**, *132*, 18643–18647.
- [63] L. Ciano, G. J. Davies, W. B. Tolman, P. H. Walton, *Nat. Catal.* **2018**, *1*, 571–577.
- [64] E. I. Solomon, D. E. Heppner, E. M. Johnston, J. W. Ginsbach, J. Cirera, M. Qayyum, M. T. Kieber-Emmons, C. H. Kjaergaard, R. G. Hadt, L. Tan, *Chem. Rev.* **2014**, *114*, 3659–3853.
- [65] S. C. Bete, C. Würtele, M. Otte, *Chem. Commun.* **2019**, *55*, 4427–4430.
- [66] M. Otte, M. Lutz, R. J. M. Klein Gebbink, *Eur. J. Org. Chem.* **2017**, 1657–1661.
- [67] P. C. A. Buijninx, G. van Koten, R. J. M. Klein Gebbink, *Chem. Soc. Rev.* **2008**, *37*, 2716–2744.
- [68] S. C. Bete, M. Otte, *Angew. Chem. Int. Ed.* **2021**, *60*, 18582–18586; *Angew. Chem.* **2021**, *133*, 18730–18734.
- [69] R. J. Jodts, M. O. Ross, C. W. Koo, P. E. Doan, A. C. Rosenzweig, B. M. Hoffman, *J. Am. Chem. Soc.* **2021**, *143*, 15358–15368.
- [70] W. Peng, X. Qu, S. Shaik, B. Wang, *Nat. Catal.* **2021**, *4*, 266–273.
- [71] S. C. Bete, L. K. May, P. Woite, M. Roemelt, M. Otte, *Angew. Chem. Int. Ed.* **2022**, *61*, e202206120; *Angew. Chem.* **2022**, *134*, e202206120.
- [72] Y. Makita, K. Ikeda, K. Sugimoto, T. Fujita, T. Danno, K. Bobuatong, M. Ehara, S. Fujiwara, A. Ogawa, *J. Organomet. Chem.* **2012**, *706–707*, 26–29.
- [73] O. Perraud, A. B. Sorokin, J.-P. Dutasta, A. Martinez, *Chem. Commun.* **2013**, *49*, 1288–1290.
- [74] D. Zhang, J.-C. Mulatier, J. R. Cochrane, L. Guy, G. Gao, J.-P. Dutasta, A. Martinez, *Chem. Eur. J.* **2016**, *22*, 8038–8042.
- [75] D. Zhang, K. Jamieson, L. Guy, G. Gao, J.-P. Dutasta, A. Martinez, *Chem. Sci.* **2017**, *8*, 789–794.
- [76] A. Martinze, J.-P. Dutasta, *J. Catal.* **2009**, *267*, 188–192.
- [77] S. A. Ikbali, C. Colomban, D. Zhang, M. Delecluse, T. Brotin, V. Dufaud, J.-P. Dutasta, A. B. Sorokin, A. Martinez, *Inorg. Chem.* **2019**, *58*, 7220–7228.
- [78] V. Steinmetz, F. Couty, O. R. P. David, *Chem. Commun.* **2009**, 343–345.
- [79] G. Qiu, P. Nava, A. Martinez, C. Colomban, *Chem. Commun.* **2021**, *57*, 2281–2284.
- [80] Y. Ning, Y. Huo, H. Xue, Y. Du, Y. Yao, A. C. Sedgwick, H. Lin, C. Li, S.-D. Jiang, B.-W. Wang, S. Gao, L. Kang, J. L. Sessler, J.-L. Zhang, *J. Am. Chem. Soc.* **2020**, *142*, 10219–10227.
- [81] H. Zhang, J.-H. Wu, H.-Z. Xue, R. Zhang, Z.-S. Yang, S. Gao, J.-L. Zhang, *Chem. Sci.* **2022**, *13*, 8979–8988.
- [82] T. Murase, S. Sato, M. Fujita, *Angew. Chem. Int. Ed.* **2007**, *46*, 5133–5136; *Angew. Chem.* **2007**, *119*, 5225–5228.
- [83] S. Kassem, T. van Leeuwen, A. S. Lubbe, M. R. Wilson, B. L. Feringa, D. A. Leigh, *Chem. Soc. Rev.* **2017**, *46*, 2592–2621.
- [84] N. Koumura, R. W. J. Zijstra, R. A. van Delden, N. Harada, B. L. Feringa, *Nature* **1999**, *401*, 152–155.
- [85] M. Krick, J. Holstein, C. Würtele, G. H. Clever, *Chem. Commun.* **2016**, *52*, 10411–10414.
- [86] Y. Qin, J. Xiong, Q. Li, Y. Zhang, M.-H. Zeng, *Chem. Eur. J.* **2022**, *28*, e202201821.
- [87] K. Suzuki, M. Kawano, S. Sato, M. Fujita, *J. Am. Chem. Soc.* **2007**, *129*, 10652–10653.
- [88] D. Fujita, K. Suzuki, S. Sato, M. Yagi-Utsumi, Y. Yamaguchi, N. Mizuno, T. Kumasaka, M. Takata, M. Noda, S. Uchiyama, K. Kato, M. Fujita, *Nat. Commun.* **2012**, *3*, 1093.
- [89] D. Fujita, R. Suzuki, Y. Fujii, M. Yamada, T. Nakama, A. Matsugami, F. Hayashi, J.-K. Weng, M. Yagi-Utsumi, M. Fujita, *Chem* **2021**, *7*, 2672–2683.
- [90] N. Schäfer, M. Bühler, L. Heyer, M. I. S. Röhr, F. Beuerle, *Chem. Eur. J.* **2021**, *27*, 6077–6085.
- [91] E. O. Bobylev, D. A. Poole III, B. de Bruin, J. N. H. Reek, *Chem. Sci.* **2021**, *12*, 7696–7705.
- [92] C. J. Bruns, D. Fujita, M. Hoshino, S. Sato, J. F. Stoddart, M. Fujita, *J. Am. Chem. Soc.* **2014**, *136*, 12027–12034.
- [93] X. Tang, H. Jiang, Y. Si, N. Rampal, W. Gong, C. Cheng, X. Kang, D. Fairen-Jimenez, Y. Cui, Y. Liu, *Chem* **2021**, *7*, 2771–2786.
- [94] E. G. Percástegui, *Chem. Commun.* **2022**, *58*, 5055–5071.
- [95] B. P. Burke, W. Grantham, M. J. Burke, G. S. Nichol, D. Roberts, I. Renard, R. Hargreaves, C. Cawthorne, S. J. Archibald, P. J. Lusby, *J. Am. Chem. Soc.* **2018**, *140*, 16877–16881.
- [96] R. Mobili, G. Preda, S. La Cognata, L. Toma, D. Pasini, V. Amendola, *Chem. Commun.* **2022**, *58*, 3897–3900.
- [97] A. Platzek, S. Juber, C. Yurtseven, S. Hasegawa, L. Schneider, C. Drechsler, K. E. Ebbert, R. Rudolf, Q.-Q. Yan, J. J. Holstein, L. V. Schäfer, G. H. Clever, *Angew. Chem. Int. Ed.* **2022**, *61*, e202209305; *Angew. Chem.* **2022**, *134*, e202209305.
- [98] K. Wu, E. Benchimol, A. Baksi, G. H. Clever, *ChemRxiv* **2023**, DOI: 10.26434/chemrxiv-2023-5gb4q.
- [99] R.-J. Li, J. Tassarolo, H. Lee, G. H. Clever, *J. Am. Chem. Soc.* **2021**, *143*, 3865–3873.
- [100] D. Preston, J. E. Barnsley, K. C. Gordan, J. D. Crowley, *J. Am. Chem. Soc.* **2016**, *138*, 10578–10585.
- [101] Y. Liu, S.-H. Liao, W.-T. Dai, Q. Bai, S. Lu, H. Wang, X. Li, Z. Zhang, P. Wang, W. Lu, Q. Zhang, *Angew. Chem. Int. Ed.* **2023**, *62*, e202217215; *Angew. Chem.* **2023**, *135*, e202217215.
- [102] L. R. Holloway, P. M. Bogie, Y. Lyon, R. R. Julian, R. J. Hooley, *Inorg. Chem.* **2017**, *56*, 11435–11442.
- [103] M. Zhu, S. Han, J. Liu, M. Tan, W. Wang, K. Suzuki, P. Yin, D. Xia, X. Fang, *Angew. Chem. Int. Ed.* **2022**, *61*, e202213910; *Angew. Chem.* **2022**, *134*, e202213910.

Manuscript received: January 6, 2023
Revised manuscript received: February 24, 2023
Accepted manuscript online: March 3, 2023